Contrib Mineral Petrol (2001) 140: 577–587
DOI 10.1007/s004100000201

L. N. Kogarko · G. Kurat · T. Ntaflos

Carbonate metasomatism of the oceanic mantle beneath Fernando de Noronha Island, Brazil

Received: 26 January 2000 / Accepted: 11 September 2000 / Published online: 15 November 2000
© Springer-Verlag 2000

Abstract Evidence is presented for a carbonate-immiscibility phenomena in the upper mantle based on data from a set of strongly metasomatized xenoliths in a basanitic lava flow from Fernando de Noronha Island (southwest Atlantic). A petrological and geochemical study of lherzolitic and harzburgitic xenoliths reveals that the oceanic mantle of this region has been affected by very strong carbonate metasomatism. The metasomatism led to wehrlitization of the primary mantle mineral assemblage (ol, opx, sp). The wehrlitization was the result of interaction between a possibly ephemeral sodic dolomitic melt or fluid with the mantle peridotite according to the following reactions, which include sodic components:

$$4MgSiO_3 + CaMg(CO_3)_2 = 2Mg_2SiO_4 + CaMgSi_2O_6 + 2CO_2$$

$$3CaMg(CO_3)_2 + CaMgSi_2O_6 = 4CaCO_3 + 2Mg_2SiO_4 + 2CO_2$$

The olivine has abundant micro-inclusions consisting of Na–Al–Si-rich glass, Fe, Ni and Cu-monosulfide, Ca-rich carbonate and dense CO_2. The interrelationships between the glass, sulfide and carbonate inclusions permit speculation that silicate, sulfide, and Ca-rich carbonatite melts were in equilibrium with each other and originated from partial melting of metasomatized and wehrlitized peridotite underneath Fernando de Noronha Island. These results support a two-stage model of Ca-rich carbonatite formation: first stage – metasomatic wehrlitization and carbonatization of mantle rocks; second stage – partial melting of the carbonate-bearing wehrlitic rock resulting in the formation of immiscible silicate, sodic carbonate and sulfide liquids and the ultimately generation of calciocarbonatites.

L. M. Kogarko (✉)
Vernadsky Institute of Geochemistry and Analytical Chemistry, Kosygin, str. 19, Moscow, 117975, Russia
E-mail: kogarko@geokhi.ru

G. Kurat
Naturhistorisches Museum, Postfach 417, 1014 Vienna, Austria
E-mail: gero.kurat@univie.ac.at
Tel.: +43-1-52177264

T. Ntaflos
Institute of Petrology, University of Vienna, Althanstrasse 9, 1090 Vienna, Austria
E-mail: theodoros.ntaflos@univie.ac.at
Fax: +43-1-31336785

Introduction

Mantle metasomatism is a very powerful process of global geochemical differentiation. The large-scale mass transportation in the upper mantle is closely connected with the origin of alkaline and carbonatitic magmatism. For example, isotopic data for Kola Peninsula alkaline rocks, carbonatites and related gigantic rare metal deposits suggest that they originated from a relatively depleted mantle source ($\epsilon Nd = 4.5$; $Sr^{87}/Sr^{86} = 0.7035$–0.7038 (Kogarko et al. 1983; Kogarko 1996). A similar depleted signature was also reported for oceanic Cape Verde carbonatites that are likewise strongly enriched in rare earth and rare incompatible elements (Silva et al. 1981; Kogarko 1993) So there is a paradox: on the one hand these rocks are extremely enriched in rare elements and on the other they have an isotopic signature corresponding to mantle rocks depleted in trace elements. The enormous concentration of rare elements in the alkaline rocks and carbonatites of these regions is mostly related to large-scale processes of mantle metasomatism confined to a very narrow time span, so the primary isotopic signature of the depleted rocks remains unchanged.

Metasomatism, cryptic and patent, has been observed in upper mantle rocks worldwide (Menzies and Hawkesworth 1987; Ionov et al. 1993; Yaxley et al. 1998). The metasomatizing agent appears to be either highly mobile silicate and/or carbonate liquids or fluids dominated by CO_2 or H_2O. Metasomatic processes can permit the precipitation of one mineral at a time, offering a direct way for the formation of monomineralic upper

mantle rocks (Hess 1960; Loomis and Gottschalk 1981; Kurat et al. 1993).

Various researchers have suggested that primary carbonate melts could be efficient metasomatizing agents, forming second generation clinopyroxene, olivine and spinel and minerals enriched in light rare earth elements (LREEs) such as apatite, krishtonite, etc. (Yaxley et al. 1991, 1998; Dautria et al. 1992; Ionov et al. 1993, 1994; Rudnick et al. 1992; Kogarko et al. 1995). Recently, we demonstrated (Kogarko et al. 1995) that the sub-oceanic harzburgitic mantle of Montana Clara Island (Canary Archipelago) had been metasomatized by primary dolomitic melt following the reaction:

enstatite + dolomite = forsterite + diopside + CO2

At Montana Clara Island the carbonatized and wehrlitized mantle was partially melted during adiabatic decompression, which resulted in the formation of three immiscible liquids (sulfide, carbonate, and silicate). This was the first reported occurrence of a primary magma within peridotites having the composition of calciocarbonatite. We proposed that the investigated Montana Clara assemblage represented a micro-model for the generation of Ca-rich carbonatitic magmas during partial melting of carbonatized and metasomatized oceanic mantle.

Later, Yaxley et al. (1998) reported a very similar mineral assemblage in mantle nodules hosted by the Newer Volcanics of southeastern Australia. In this assemblage, nearly pure primary calcite is found mostly as rounded blebs within the silica-rich glass patches in association with clinopyroxene and second generation olivine. The study provided evidence for the existence of sodic dolomitic melts in the lithosphere beneath southeastern Australia. These melts are believed to have been the major agent of mantle metasomatism of originally harzburgite-dominated, depleted and refractory lithospheric material. At the initial stages of this process cryptically metasomatized (enriched in incompatible trace-element) harzburgites and lherzolites formed. However, when the proportion of infiltrating dolomite melt exceeded 6–12%, reaction enstatite + dolomite = forsterite + diopside + CO_2 (at 1.5–2 GPa) proceeded to completion and wehrlites with apatite, amphibole, phlogopite and calcite were produced. Yaxley et al. (1998) suggested that the calcite in the Australian assemblage represents cumulus crystals.

Seifert and Thomas (1995) found wehrlite xenoliths in the Grosser Winterberg tephrite (Germany) that contain grain-boundary melt pockets consisting of silicate glass with immiscible (Ca, Fe, Mg)-carbonate globules. They interpreted the generation of the Ca-rich carbonate melt as a result of mantle metasomatism by CO_2-dominated fluids. Pyle and Haggerty (1994) described an assemblage of globules of Ca-rich carbonate and Na–Al glass in metasomatized eclogite xenoliths from South African kimberlites. They attributed the silicate–carbonate textural relationships to liquid immiscibility in the upper mantle. Other workers have found Mg-rich carbonate in mantle peridotites from Spitsbergen in association with silicate glasses and have interpreted these assemblages as evidence of liquid immiscibility (Amundsen 1987; Ionov et al. 1993).

These examples of carbonate-silicate liquid immiscibility in the upper mantle appear to be supported by the experimental data of Koster van Groos (1975), Freestone and Hamilton (1980), Kjarsgaard and Hamilton (1989), Baker and Wyllie (1990), and Hamilton and Kjarsgaard (1993). These experimental studies have demonstrated the immiscibility between Na-rich carbonatite and silicate magmas over a wide range of pressures (2–25 kbar).

However, Lee and Wyllie (1994, 1996) have pointed out a number of limitations to this hypothesis. They presented evidence that crystalline calcite can grow in silicate–carbonate liquids with a remarkably rounded morphology simulating the characteristics of melts. On the basis of the available experimental evidence they concluded that the compositions of carbonate aggregates situated in the aluminosilicate glass of mantle xenoliths makes these aggregates unlikely candidates for Ca-rich carbonate liquids immiscible with silicate liquids. Recently, Ionov (1998) presented new information for Ca-rich carbonates in mantle xenoliths from Mongolia and Spitsbergen. The low alkali contents in the carbonate pockets are likely to be consistent with their origin as crystal cumulates rather than as quenched liquids. But, Ionov (1998) pointed out that "the origin of the textural relationships between the carbonate globules and silicate glass remains enigmatic".

The genesis of Ca-rich carbonatitic melts in the upper mantle is still unresolved, and new mineralogical observations on the interrelationships between carbonate and silicate material in deep-seated xenoliths remain very important. In this paper we present new evidence for carbonate–silicate–sulfide liquid immiscibility based on data from a set of strongly metasomatized xenoliths in a basanitic lava flow from Fernando de Noronha Island (southwest Atlantic).

Geological setting

Fernando de Noronha Island is situated in the southwest Atlantic, 345 km off the coast of Brazil. The island has an area of 16.9 km^2 and consists of three complexes of intrusive and effusive rocks: the Remedious complex, the Quixaba formation, and the Sao Jose formation and (Almeida 1958; Mitchel-Thome 1970). The oldest formation, the Remedius complex, is represented by phonolitic, trachytic, and alkalitrachytic plugs, dykes and stocks, together with some extrusive pyroclastic rocks including agglomerates, breccias, lapilli-tuffs and ash. The composition of the pyroclastic material is mostly phonolitic and trachytic. Dykes of the Remedius complex include different types of foidite, basanite, tephrite and phonolite. The second oldest Quixaba formation overlaps the Remedius rocks in two isolated occurrences. In marked contrast to the Remedius formation, Quixaba rocks are almost entirely extrusive and of olivine nephelinitic composition. The youngest rocks of Fernando de Noronha Island are those of the Sao Joze formation, which are of basanitic composition. They

crop out on the islets of Chapeo de Nordeste and Sao Joze (Almeida 1958; Mitchel-Thome 1970). The basanite lava flows of these islets contain large amount of upper mantle xenoliths. The xenoliths were first noted by Almeida (1958) and later briefly described by Meyer and Svisero (1987) who give some information on the mineralogy of these xenoliths.

Analytical methods

Minerals were analyzed in Vienna University using a Cameca SX100 electron microprobe operated at 15 kV accelerating voltage and 20 nA beam current. Natural and synthetic minerals were used as standards for calibration. Counting times were 20 s for all elements. Ca in olivine was analyzed using pure wollastonite as a primary standard and San Carlos olivine as a secondary standard at 20 kV accelerating voltage and 40 nA beam current. Counting times were 100 s for both peak and background positions. To prevent loss of alkalis during analysis of glasses and glass inclusions we decreased the counting time to 15 s, but even in these cases some alkalis might have been lost. A Pouchou and Pichoir correction was applied to all data.

Rare earth element abundance have been determined for 15 representative samples by instrumental neutron-activation analysis (INAA; Wanke et al. 1973; Kolesov 1994) in the Vernadsky Institute of Geochemistry and Analytical Chemistry using reactor facilities provided by Moscow Engineering Physical Institute.

Textural relationships and chemical compositions

We collected mantle xenoliths from the Sao Jose formation on the islets of Chapeo de Nordeste and Sao Joze during a 1991 oceanic expedition by the Scientific Vessel *Academician Boris Petrov*. Most xenoliths are within the size range 0.5–25 cm and, very rarely, up to 35 cm. The xenoliths are all ultramafic and compositionally form two main groups: (1) spinel lherzolites and harzburgites (predominant), and (2) pyroxene-rich rocks and wehrlites (less common). We found no garnet-bearing ultramafitites.

Most of the spinel lherzolites and harzburgites have granoblastic texture. Xenoliths with porphyroclastic texture are less common. The modal proportions of the four principal minerals are variable: olivine −65–80 vol%, orthopyroxene −7–25 vol%, and clinopyroxene and spinel −0.5–10 vol%. Pyroxene-rich ultramafitites and wehrlites are rare. The proportions of clinopyroxene, olivine and spinel in the pyroxene-rich peridotites are highly variable.

Both types of rocks show clear evidence for patent metasomatism characterized by the presence of Ca-rich carbonate, apatite, and second generation assemblages consisting of fine-grained olivine (5–40 μm), clinopyroxene (1–35 μm), spinel (1–15 μm), carbonate (10–200 μm), glass (up to 1–2 mm) and sulfides (0.5–10 μm). In one xenolith we found very small (7-μm) crystals of kirschsteinite confined to healed micro-fractures in first generation olivine filled with carbonate in close association with low-density fluid inclusions (Table 1). First generation olivine, orthopyroxene, spinel, and clinopyroxene are very coarse-grained, sometimes up to 3–5 mm across. They are crossed by numerous veinlets of a fine-grained assemblage, which surrounds and replaces first generation minerals, especially orthopyroxene (Fig. 1A, E, F). These fine-grained zones contain second generation clinopyroxene, olivine, carbonate, glass, apatite, armalcolite, and kirschteinite. In some cases, second generation clinopyroxene replaces second generation olivine (Fig. 1A, F).

The compositions of first generation olivine, orthopyroxene, clinopyroxene, and spinel (Table 1) are typical of upper mantle lherzolites. Second generation olivines are richer in calcium (up to 0.27 wt% CaO) than the

Table 1 Chemical compositions of bulk rocks, minerals and melt inclusions

Sample	SiO_2	TiO_2	Al_2O_3	FeO	MnO	Cr_2O_3	NiO	MgO	CaO	Na_2O	K_2O	ZnO	CuO	S	Sum
Nodule FN-20	44.31	0.16	2.72	8.59	0.14	0.23	–	40.04	2.16	0.3	0.11	–	–	–	98.76
Olivine (I)	40.94	–	0.02	9.89	0.14	0.02	0.33	48.54	0.08	0.01	–	–	–	–	99.97
Olivine (II)	40.63	0.05	0.01	10.13	0.17	0.06	0.20	47.48	0.18	0.04	–	–	–	–	98.95
Orthopyroxene (1)	56.35	0.48	3.99	6.76	0.22	0.67	0.04	30.46	0.64	–					99.69
orthopyroxene (I)	54.12	0.06	4.69	6.26	0.09	0.54	0.10	32.06	0.81	0.09	–	–	–	–	98.82
Clinopyroxene (I)	51.17	0.21	5.67	3.44	0.08	0.90	0.02	15.75	18.68	1.22	–	–	–	–	97.14
Clinopyroxene (II)	53.09	1.00	1.19	2.89	0.03	1.20	0.08	18.05	22.69	0.55	–	–	–	–	100.77
Clinopyroxene (II)	41.07	0.11	5.76	4.72	0.00	0.89	0.04	15.69	28.49	2.33	0.00	0.00	0.00	0.00	99.11
Spinel (I)	0.06	0.12	45.54	17.84	0.11	16.23	0.32	17.84	–	0.01	–	–	–	–	98.08
Armalcolite	0.06	71.18	1.99	11.47	0.10	2.48	–	10.99	0.07	–	–	–	–	–	98.34
Carbonate inclusion	2.92	0.71	0.96	1.30	0.00	0.00	0.00	4.26	45.50	0.45	0.36	–	–	–	56.46
Carbonate	0.32	–	–	0.31	0.03	–	0.03	1.00	52.43	0.11	–	–	–	–	54.23
Glass inclusion	57.47	1.02	25.42	1.56	–	–	–	–	0.97	9.04	3.87	–	–	–	99.35
Interstitial glass	55.45	2.35	22.17	1.17	0.56	0.00	0.00	3.13	1.11	8.18	4.88	0.00			99.00
Interstitial glass	53.76	3.60	19.00	0.79	0.90	0.15	0.29	6.12	2.10	8.04	5.27	0.00			100.02
Interstitial glass	64.23	0.50	18.96	0.31	0.00	0.00	0.10	0.00	1.27	9.19	4.51	0.00			98.97
Sulfide inclusion[a]	–	0.01	0.01	32.65	0.03	–	32.50	–	–	0.11	–	–	–	33.97	99.28
Sulfide in carbonate inclusion[a]	–	–	–	33.27	–	–	31.75	–	–	–	–	2.62	0.82	31.43	99.89
Kirschsteinite	30.92	0.08	0.31	39.79	0.40	0.00	0.12	15.81	11.37	0.00	0.00	–	–	–	98.80
Cpx (host lava)	47.44	2.51	4.46	6.76	0.39	0.02	0.19	12.33	25.23	0.65	–	–	–	–	99.98

[a] Analyses of sulfides are presented as wt% of elements

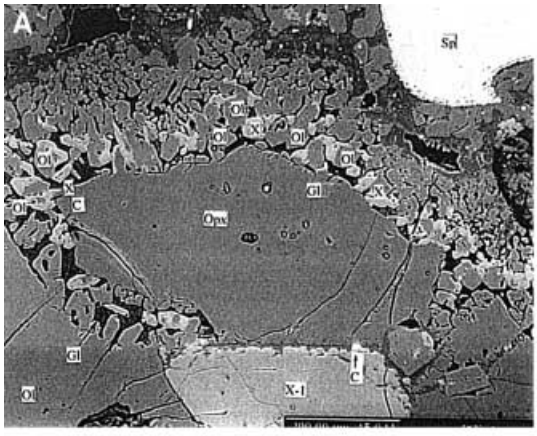
A
Spl
Ol
X
Opx
Gl
C
X-1

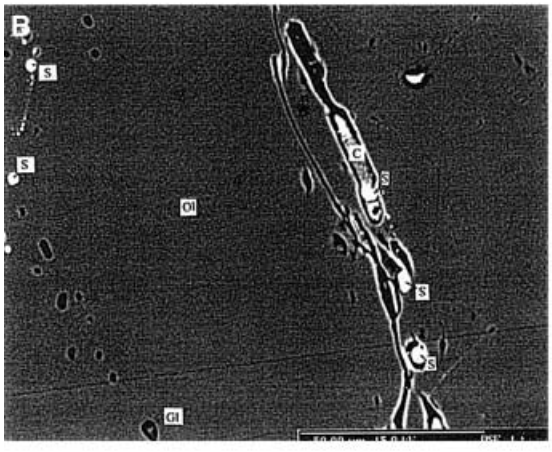
B
S
Ol
C
Gl

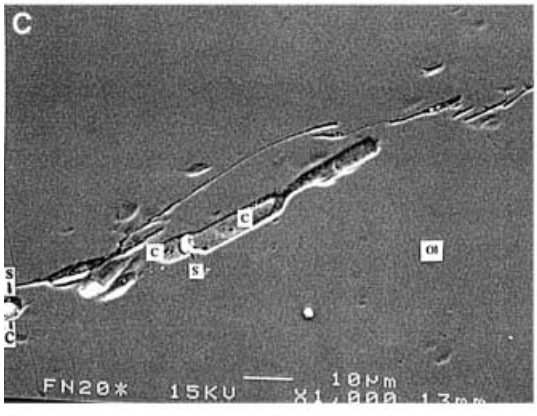
C
Ol
S
C
FN20*
15KU
10μm

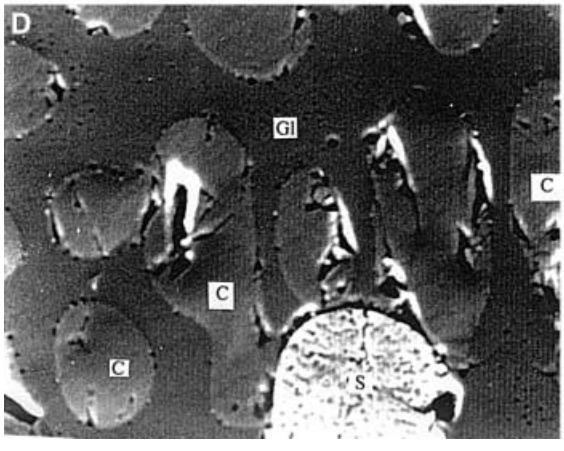
D
Gl
C
S

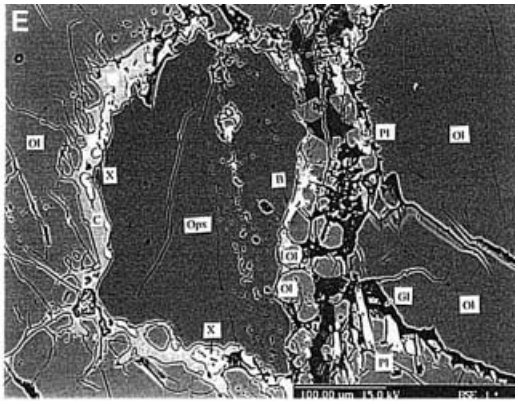
E
Ol
X
Pl
Opx
Gl


F
Gl
X
Ol

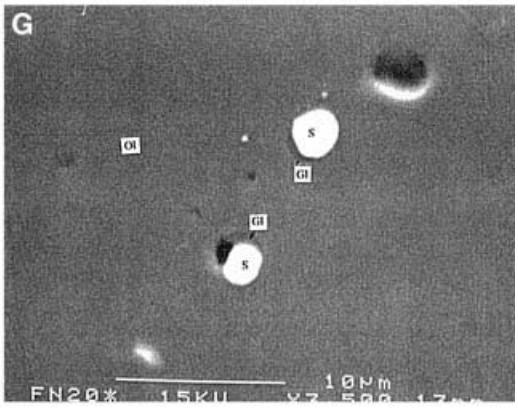
G
Ol
S
Gl
FN20*
15KU
10μm

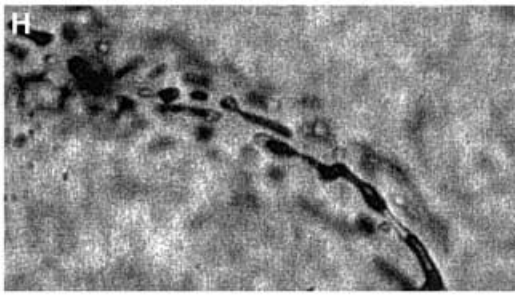
H

◀

Fig. 1 **A** Back-scattered electron image of orthopyroxene being replaced by fine-grained mineral assemblage. *Opx* Orthopyroxene; *Ol* olivine; *X–1* clinopyroxene 1 generation; *X* clinopyroxene 2 generation; *Gl* glass; *C* carbonate; *Sp* spinel 1 generation. **B** Back-scattered electron image of inclusions in the first generation olivine. *Bright white* sulfide melt inclusions (*S*); *white* carbonate inclusion containing a sulfide globule (*C*), inclusion is partly leached; *gray* inclusions of trachytic phonolitic glass (*G*), olivine. **C** Back-scattered electron image of carbonate–sulfide inclusion in olivine. *C* Carbonate; *S* sulfide; *Ol* olivine. **D** Back-scattered electron image of a melting experiment product, T = 1220 °C, p = 8 kbar. Sulfide–silicate–carbonate immiscibility. *S* Sulfide liquid; *C* carbonate liquid; *Gl* glass, silicate liquid; magnification ×370 (Kogarko and Slutsky 2000). **E** Back-scattered electron image of orthopyroxene being replaced by fine-grained mineral assemblage. *Opx* Orthopyroxene; *Ol* olivine; *X* clinopyroxene; *Gl* glass; *C* carbonate; *B* barian–celestine; *Pl* plagioclase. **F** Back-scattered electron image of reaction zone between orthopyroxene and carbonate melt. *C* Carbonate veinlet and carbonate blebs; *Opx* orthopyroxene; *X* clinopyroxene; *Gl* glass; *Sp-2* armalcolite. **G** Back-scattered electron image of silicate–sulfide inclusions in olivine. *Gl* Glass; *S* sulfide. **H** Late liquid–gas CO_2 inclusions in olivine

primary olivines (0.06–0.08 wt%). Second generation clinopyroxenes are more Ca- and Mg-rich and less aluminous and sodic compared with the original clinopyroxenes.(Fig. 2). However, in some second generation clinopyroxenes, the sodium concentration reaches 2.33 wt% Na_2O, which is close to that of the primary clinopyroxenes (Table 1).

Armalcolite is common in the second generation assemblage in close association with glass. Carbonate fills irregularly-shaped, round or vermicular pockets with sharp curvilinear boundaries with the glass, and is closely associated with second generation clinopyroxene and olivine situated in reaction zones. Polycrystalline (according to optical investigations) carbonates are usually partly leached and fill veinlets closely connected with metasomatic zones (Fig. 1F). In one reaction aureole, we found Ba–Sr sulfate (barian celestine) in association with calcite, second generation clinopyroxene, spinel, olivine, glass and primary orthopyroxene (Fig. 1E).

In some rocks networks of veinlets are present (up to 2 μm wide and up to 100 μm long), which are filled only with Ca-rich carbonate. The carbonate composition is that of a Mg-bearing calcite with an atomic Ca/(Mg + Ca + Fe + Na) ratio in the range of 0.85–0.96 and minor amounts of Si, Fe, Al, and Na (Table 1).

Interstitial patches of brownish Na–Al glass incorporate second generation olivine, clinopyroxene, spinel, and carbonate. Quench crystals of Cl-bearing apatite (Cl content is up to 0.65 wt%) and rutile are also present in the glass. The composition of the glass is variable (Fig. 3) ranging from that of basaltic andesite to that of highly evolved trachytic, phonolitic, and dacitic melts. In some cases, the glasses are partly crystallized and contain quench plagioclase and potassium feldspar. Very similar glass compositions have also been reported in upper mantle xenoliths from many other continental and oceanic localities (Edgar et al. 1989; Yaxley et al. 1991, 1998; Dautria et al. 1992; Schiano et al. 1992; Hauri et al. 1993; Ionov et al. 1993; Kogarko et al. 1995; Ionov 1998; Varela et al. 1999).

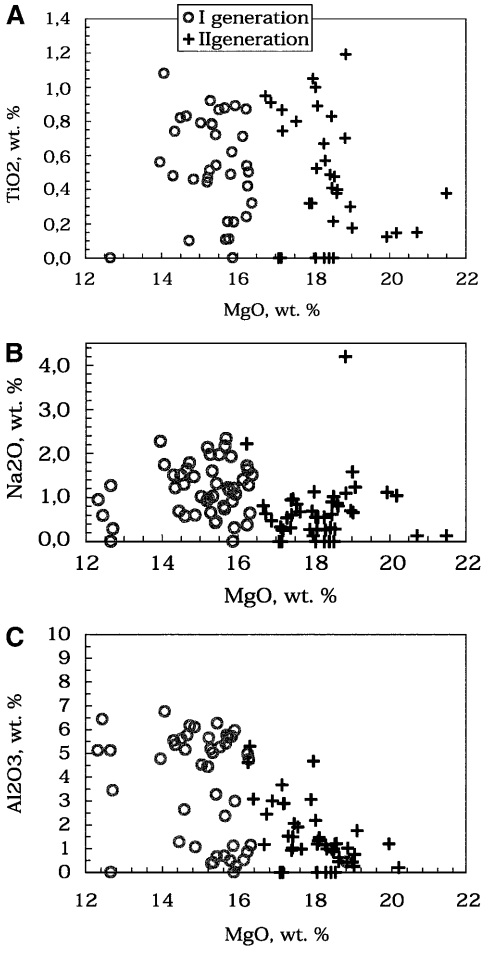

Fig. 2 Plots of oxides vs wt% MgO comparing 1 and 2 generation clinopyroxenes. **A** MgO–TiO_2; **B** MgO–Na_2O; **C** MgO–Al_2O_3

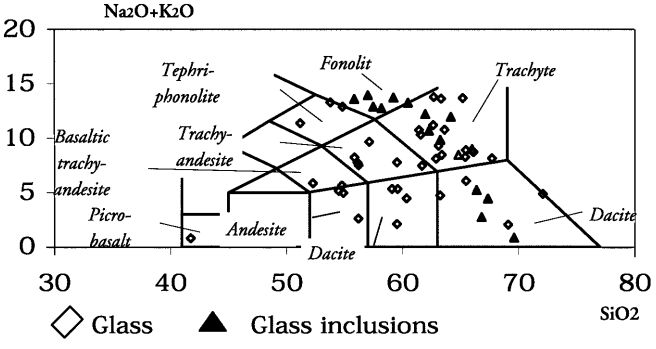

Fig. 3 The chemical composition of glass inclusions in olivine and glass from reaction zones in Fernando de Noronha xenoliths projected into the alkali-silica diagram

Glasses often include Fe–Ni sulfide globules with compositions typical for primary mantle sulfides (Table 1). The globules mostly contain nickeliferous pyrrhotites, pentlandite or possibly monosulfide solid solutions with minor amounts of Cu and Co.

The olivines contain abundant micro-inclusions filled with Na–Al silicate glass, Fe, Ni, and Cu monosulfide, carbonate, and CO_2. The silicate glass inclusions form blebs of round, oval or negative crystal shapes (0.5–30 μm). They are isotropic, but in rare cases show very weak birefringence. Occasionally, these micro-inclusions also contain droplets of Fe–Ni sulfides or a bubble (Fig. 1B, G). The glass of these inclusions usually has a chemical composition similar to that of peralkaline phonolites, trachytes or dacites (Table 1).

Sulfide micro-inclusions with sizes from 0.5 to 5 μm form accumulations sometimes containing linear arrays of inclusions varying from spheres to equant negative crystals (Fig. 1B, G). The sulfide inclusions are dominantly nickeliferous mono-sulfide with minor amounts of Co and Cu. In one rock we found a pyrrhotite–chalcopyrite association. In some Fe–Ni sulfide inclusions we noted up to 2.62 wt% Zn in nickeliferous monosulfide. To the best of our knowledge, Zn has not previously been reported from upper mantle sulfides.

Some micro-inclusions are filled with polyphase assemblages containing silicate glass and monosulfide with curved boundaries between phases (Fig. 1G).

The carbonate micro-inclusions form elongated rods, tubes or negative crystals. They usually show traces of leaching of carbonate material (Fig. 1B, C). In some inclusions, Ni–Fe-sulfide (Table 1) are enclosed in the carbonate and partly leached carbonate with curved menisci (Fig. 1B, C). Glass, sulfide and carbonate inclusions are closely related and confined to the same planes in the olivine crystals (Fig. 1B), testifying to a simultaneous trapping of these micro-inclusions as droplets of melt.

All major silicate phases of the rocks are rich in CO_2 inclusions, especially olivine (Fig. 1H).

The bulk chemical composition of these xenoliths reveals the typical covariation pattern shown by the majority of mantle material (Fig. 4).

REE analyses of investigated xenoliths are shown in Fig. 5. Chondrite-normalized REE patterns of the investigated peridotites in the majority of cases exhibit complex S-like shapes: the normalized abundances drop from La to Pr, then increase with atomic number to reach a maximum at Tb and subsequently decrease to Lu. Some specimens also exhibit a very weak negative Eu anomaly.

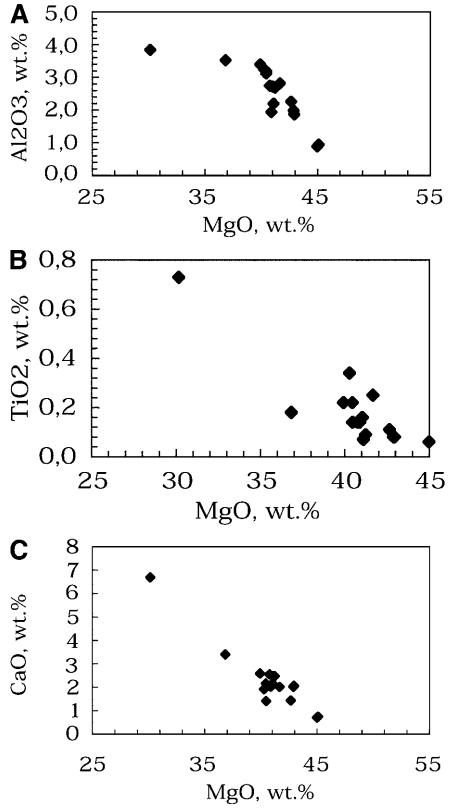

Fig. 4 Co-variations of MgO–CaO, MgO–Al_2O_3, and MgO–TiO_2 in xenoliths from Fernando de Noronha

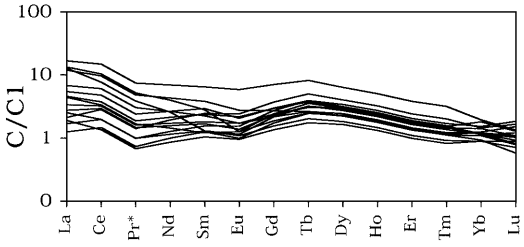

Fig. 5 The abundances of rare earth elements in upper mantle xenoliths from Fernando de Noronha normalized to CI chondrite (data from Taylor and McLennan 1985)

Discussion

Metasomatic interaction between dolomite melt and oceanic mantle

The close connection of alkaline and carbonatitic magmatism with mantle metasomatism and fluid migration initiated by rifting is widely accepted. It is generally assumed on the basis of isotope (Menzies and Murthy 1980; Menzies and Wass 1983), trace element (Wass and Rogers 1980; Kogarko 1996) and experimental studies (Wyllie 1989; Dalton and Wood 1993) that mantle metasomatism is an inevitable precursor for the generation of alkaline and carbonatitic magmas. A small degree of partial melting of carbonate-bearing peridotite at pressures above 20 kbar generates dolomitic (Wyllie and Huang 1976; Wyllie 1987) or alkali-rich dolomitic melts (Wallace and Green 1988; Thibault et al. 1992), which could be a very active metasomatizing agent forming carbonate-bearing wehrlitic assemblages: clinopyroxene, olivine, spinel and carbonate (Yaxley et al. 1991; Ionov et al. 1993, 1994; Rudnick et al. 1992; Kogarko et al. 1995). Dalton and Wood (1993) showed that, at lower pressure (15 kbar), Ca-rich carbonatite melt (with Ca/

(Ca + Mg + Fe + Na) ratios up to 0.96) could be produced in the mantle as a result of wallrock reaction of less calcic melts with a wehrlitic assemblage. The Mg/Fe ratio in carbonate also increases during this process.

Textural evidence and the mineral compositions of the investigated xenoliths indicate very active metasomatic interaction between primary dolomite melt (or fluid) and oceanic mantle below Fernando de Noronha following schematic reactions, which include sodic components:

$$\underset{orthopyroxene}{2Mg_2Si_2O_6} + \underset{melt}{CaMg(CO_3)_2} = \underset{olivine}{2Mg_2SiO_4} + \underset{clinopyroxene}{CaMgSi_2O_6} + \underset{fluid}{2CO_2} \quad (1)$$

$$\underset{melt}{3CaMg(CO_3)_2} + \underset{clinopyroxene}{CaMgSi_2O_6} = \underset{melt}{4CaCO_3} + \underset{olivine}{2Mg_2SiO_4} + \underset{fluid}{CO_2} \quad (2)$$

A second generation of minerals and numerous CO_2 inclusions occurring in olivine, and less often in other minerals, appears to have formed as a result of these reactions. Mineral chemical features of the second generation assemblage (more Ca and Mg in clinopyroxene and high Ca contents of olivine) also imply that the metasomatic agent was enriched in Ca and Mg and highly depleted in silica, being unstable in the presence of orthopyroxene and in equilibrium with more Ca- and Mg-rich clinopyroxene and Ca-enriched olivine (Table 1). In some cases second generation olivine is clearly replaced by second generation clinopyroxene (Fig. 1F), which probably reflects the closeness of the system to univariant equilibrium described by reaction (2). Fluctuation of $p(CO_2)$ may shift this reaction to the right or to the left. Using two-pyroxene geothermometry and Ca-in-olivine geobarometry (Brey and Koehler 1990), the lower equilibration temperature limit for the second generation minerals is found to be 1050–1105 °C with a pressure of 11–14 kbar. This pressure is close to that at which the Dalton and Wood (1993) experiments producing high-calcium carbonate melts with high Mg-number were done. The calcium-rich carbonate confined to the wehrlite veinlets of the Fernando de Noronha xenoliths has very high Ca\(Ca + Mg + Fe + Na) (0.84–0.91) and Mg\(Mg + Fe) ratios (0.81–0.86; Table 1). Our calculations show the equilibration pressure and temperature ranges for the first generation of minerals, which were formed before the metasomatic event to be 18–23 kbar and 1255–970 °C. Such values may imply that the uplift of mantle material was simultaneous with carbonatite metasomatism and CO_2 degasation, in agreement with our data on CO_2 micro-inclusions. These inclusions had melting temperatures of −57.1 °C, which indicates that the trapped fluid is pure CO_2 with minor amounts of other volatile species. These inclusions homogenized at –25 °C into a liquid phase with a density of 1.06 g/cm^3, estimated from CO_2 vapor–liquid equilibria (Roedder 1984). We calculated the lower limit for the trapping pressure (8.4 kbar) using the formation temperature for the second generation assemblage (1105–1050 °C). This figure show that carbonate metasomatism occurred at a depth 25–30 km after the mantle material rose from 50–70 km. Low-density CO_2 inclusions appeared to be confined to healed microfractures in host olivine (Fig. 1H). Their homogenization into a liquid phase at + 26 °C corresponds to a very low trapping pressure of about 1 kbar at 1105–1050 °C. The presence of kirschsteinite in metasomatic zones in close association with low-density CO_2 microinclusions suggests the invariant reaction:

$$Ca(Mg,Fe)Si_2O_6 + (Mg,Fe)_2SiO_4 + 2CaCO_3 = 3Ca(Mg,Fe)SiO_4 + CO_2$$

Using the temperature range of the second generation assemblage and the thermodynamic database of Shapkin et al. (1986), we obtain $p(CO_2)$ of 0.9–1.5 kbar, suggesting that the reaction may have occurred at a very shallow level of 3–5 km. We suggest that this low pressure reaction might occur in metasomatized mantle nodules on the way to the surface.

Sodium-enriched nature of metasomatic agent

In spite of the low sodium concentrations (0.1–0.7 wt% Na_2O) in the carbonate from the investigated xenoliths, we assume that the primary carbonate melt was to a large extent enriched in sodium because clinopyroxene in the second generation assemblage contains up to 2.33 wt% Na_2O. According to our calculations, based on the experimental data of Dalton and Wood (1993) and Yaxley and Green (1998), this Na_2O content of the clinopyroxene corresponds to ~30% Na_2CO_3 in the coexisting melt/fluid. Therefore, it appears likely that the metasomatic assemblage of secondary minerals was in equilibrium with a sodium-rich dolomitic melt.

It is probable that sodium was carried away by the residual low temperature fraction of the melt/fluid. The reality of this process is corroborated by experimental studies that demonstrated that alkalis are strongly partitioned into aqueous phase in equilibrium with both crystalline Na–Ca carbonates (Dernov-Pegarev and Malinin 1976) and hydrous carbonatite melts (Veksler and Keppler 2000).

REE patterns of the investigated xenoliths also appears to reflect the complex history of the mantle under Fernando de Noronha. The rocks were depleted in light rare earth elements (LREEs) in the past probably by extraction of a melt fraction. Subsequently, they experienced an enrichment in LREE because of the infiltration of sodic dolomitic melt. Substantial preferential partitioning of LREE into carbonate melts follows from experimental data (Hamilton et al. 1989).

Thus, we conclude that the primary carbonate melt or fluid which metasomatically interacted with the oceanic lithosphere below Fernando de Noronha had a sodium-bearing dolomitic carbonatite composition.

Silicate–sulfide–carbonate liquid immiscibility

It is generally accepted that glass patches in deep-seated xenoliths are mostly a result of partial melting of metasomatized mantle substrate (Yaxley et al. 1991; Schiano et al. 1992; Ionov et al. 1993; Kogarko et al. 1995; Rosenbaum et al. 1996). The strongly evolved glass composition of the Fernando de Noronha xenoliths implies that these melts were not in equilibrium with the minerals of the first generation, but, rather, formed during incongruent melting of jadeitic clinopyroxene from metasomatized veinlets (Kogarko et al. 1995).

The presence of quenched apatite and rutile in the glass may be attributed to the rapid evolution of such melts leading to saturation by these minerals. The presence of armalcolite and second generation clinopyroxene, containing sometimes up 1.3 wt% TiO_2, possibly testifies to Ti enrichment of the metasomatized zones. Metasomatic clinopyroxenes from Mongolia and Spitsbergen xenoliths in which interaction with dolomitic melts has been suggested also show higher Ti values compared with first generation clinopyroxene (Ionov 1998). Possibly Ti was introduced into the metasomatic zones. At present, experimental data point to the low solubility of Ti in carbonate-rich melts (Hamilton et al. 1989; Thibault et al. 1992; Klemme et al. 1995). However, the modeling of Ti enrichment caused by carbonate metasomatism requires more detailed knowledge of the composition of metasomatizing agents. If the metasomatizing melt (or fluid) ranges in composition between carbonate and alkali-rich silicate melts, Ti might be soluble in highly alkaline melts (Dickinson and Hess 1985). For example, Schrauder and Navon (1994) estimated, for the very alkaline carbonate melt in volatile-rich inclusions in fibrous diamonds from Jwaneng, 4.6 wt% TiO_2. Another possibility may be related to the instability of orthopyroxene containing up to 0.48 wt% TiO_2 during a carbonate metasomatic event. Therefore, orthopyroxene may substantially contribute to the budget of Ti in metasomatic zones. Partially melted first generation clinopyroxene containing up to 1.4% TiO_2 might also be the source of Ti in metasomatic veins.

Numerous sulfide micro-inclusions occur in all minerals of the rocks, especially in olivine. In some cases, glass inclusions also contain sulfides (Fig. 1G). The morphology and composition of sulfide inclusions indicate that they were trapped as droplets of immiscible melt. Andersen et al. (1987) and Amundsen (1987) have presented convincing evidence for silicate–sulfide liquid immiscibility in partially melted mantle rocks.

As noted before, the second generation phase assemblage has abundant carbonate patches with sharply curved menisci, immersed in felsic glass. These textural interrelationships between carbonate and silicate glass resemble melt immiscibility .Very close association of carbonate and silicate liquids in the investigated xenoliths can be explained by the experimental data of Minarik (1998) who reported a higher melt–solid interfacial energy for the carbonate melt than immiscible silicate liquid, resulting in conjugated migration in solid dominated assemblage.

We interpret the presence of the three different type (glass, sulfide and carbonate) of melt micro-inclusions, all confined to the same plane in olivine crystals (Fig. 1B), as unambiguous evidence of a liquid immiscibility relationship between them. The formation of the system of veins filled by carbonate in these mantle xenoliths (Fig. 1F) is very difficult to explain by the accumulation of calcite during the crystallization of silicate–carbonate melt. It is much more likely that the low-viscosity Ca-rich carbonate melt or fluid percolated through the mantle material forming a series of carbonate veins. A melt similar in composition to Ca-rich carbonatite was generated during the partial melting of wehrlitized mantle material containing calcite (Dalton and Wood 1993). The shape of the segregations of Ca-rich carbonate and the presence of three types of inclusions controlled by the same planes may also imply that the origin of Ca-rich carbonatites may be caused by the processes of liquid immiscibility. Experimental investigations suggest that liquid immiscibility plays a leading role in the genesis of carbonatites (Freestone and Hamilton 1980; Kjarsgaard and Peterson 1991). Experiments have demonstrated the presence of extensive fields of two immiscible liquids in the system $(SiO_2 + Al_2O_3 + TiO_2)$–$(MgO + FeO + CaO)$–$(Na_2O + K_2O)$–$CO_2$. The immiscibility gap expands with increasing pressure and alkali content. According to Lee and Wyllie (1996), the immiscibility gap also expands with decreasing magnesium concentration. However, Lee and Wyllie (1994, 1996) have pointed out a number of limitations to this hypothesis and maintain that there cannot be a single process responsible for the formation of all carbonatites. Their recent experimental results (Lee and Wyllie 1996) indicate that carbonate–silicate immiscibility is strongly restricted to alkali-rich melts containing at least 5% Na_2CO_3.

Our calculations based on clinopyroxene composition and experimental data of Dalton and Wood (1993) and Yaxley and Green (1998) show that up to ~30 wt% of Na_2CO_3 in the carbonatite liquid is in equilibrium with the metasomatic mineral association in wehrlites of Fernando de Noronha. Assuming equilibrium between silica-rich and carbonatite melts, one can estimate the alkali component of the latter using the partition coefficient of alkalis as determined by Hamilton et al. (1989). The calculated amounts of Na_2CO_3 fall in the range of 12–45 wt%.

Studies of crystallized melt inclusions provide new evidence for quite high alkali concentrations in carbonatite melts of some of the world's largest carbonatitic complexes – Guli, Kovdor, and Gardiner (Kogarko et al. 1991; Veksler et al. 1998). Veksler et al. (1998) have concluded that "potential carbonatite melts of Kovdor and Gardiner would be alkaline-bearing". Thus Ca-rich carbonatites may originate from primary Na-rich carbonatite melt by fractional crystallization with subsequent

wallrock reactions and loss of alkalis to the fluid phase. The existence of the natrocarbonatite volcano Oldonyo Lengai provides real evidence for the possibility of alkali-rich carbonatitic melts generation in the upper mantle.

We attribute the leaching phenomena in carbonate micro-inclusions (Fig. 1B, C) to the activity of aqueous fluids in mantle peridotites below Fernando de Noronha. From the above consideration it is thus possible to suggest that the immiscibility of carbonate, sulfide, and silicate melts took place during the partial melting of upper mantle material below the island. The original carbonate melt initially could have contained significant amounts of alkalis, which possibly were lost as result of water–alkaline carbonate melt interaction.

The immiscibility between silicate and sulfide melts has been known for many years. However, the immiscibility in carbonate–silicate–sulfide systems has been reported by us for the first time in a preliminary communication (Kogarko et al. 1998). Using a piston-cylinder apparatus, we have investigated the immiscibility in the system Ca-rich carbonate–Fe, Ni sulfide–silicate melt of phonolitic composition containing F. The experiments were made at 1250 °C and 4–15 kbar. The investigated system showed clear immiscibility: sulfide and carbonate melts were present in the form of small globules in silicate liquids (Fig. 1D). Sulfur solubility in silicate melt varies from 0.15 to 0.35 wt% and in carbonate liquid it ranges from 0.02 to 3.7 wt% depending on alkali content (Kogarko et al. 1998; Kogarko and Slutsky 2000).

Conclusions

Our investigations have revealed a very complicated multi-stage geological history for the mantle rocks below Fernando de Noronha Island. The MgO–CaO and $MgO–Al_2O_3$ co-variations in the bulk composition of the investigated rocks (Fig. 4) reflect varying degrees of partial melting during which the initial substrate lost the so-called basaltic elements: Ca, Al, Ti, Na, and incompatible trace elements. Sulfur should have been lost during this process because of the low melting temperatures of mantle sulfides. Later, this depleted mantle material was invaded by a carbonate melt/fluid with a prevailing dolomitic component that contained sodium and possibly potassium, sulfur, light rare earth elements (LREEs), titanium, strontium, barium, and phosphorous. Geochemical data demonstrate a strong influx of LREE (Fig. 5). During the metasomatic reactions partial wehrlitization and carbonatization took place along veinlets and fissures. Our calculations indicate that the metasomatic mineral assemblage probably formed at relatively low pressures (10–15 kbar), and suggest that this process was accompanied by the uplift of mantle material from depths of ~60 to 30 km. Later, during very rapid ascent of mantle material (otherwise primary carbonate would not survive), the carbonate-bearing wehrlitic mineral assemblage containing carbonate melted as result of decompression and produced a Ca- and Na-rich carbonatitic melt. In some cases three immiscible liquids – alkaline carbonate, sulfide, and silicate were formed. The last equilibration between mineral phases appears to have been reached under very low pressures of ~1 kbar at 3–5 km depth.

Comparison of our data with those published earlier (Yaxley et al. 1991; Schiano et al. 1992; Ionov et al. 1993, 1994; Rudnick et al. 1992; Kogarko et al. 1995) indicate that mantle carbonatite metasomatism is a very widespread phenomenon. However, to the best of our knowledge only three cases of carbonate metasomatism occurring in oceanic lithosphere have been reported so far: Samoa Island (Hauri et al. 1993), the Canary Archipelago (Kogarko et al. 1995), and the Cape Verde Islands (Ryabchikov et al. 1989). We suggest a close connection between carbonatite metasomatic processes in the oceanic lithosphere and the origin of very Ca-rich, silica-undersaturated and carbonatitic magmas in some of the Canary and Cape Verde islands and Fernando de Noronha.

Acknowledgements This work was financially supported by the Russian Foundation for Basic Research, project 99-05-64835, INTAS 1010-CT93-OO18, the Austrian FWF and the Austrian Academy of Sciences. We are grateful for fruitful discussions to Drs. A. Woolley and B. Close. We very much appreciate the assistance of Dr. R.E. Zartman and two referees of this paper, Drs. E.A. Dunworth and G. Yaxley, who helped substantially to improve this manuscript.

References

Almeida FFM (1958) Geology and petrology of archipelago Fernando de Noronha (in Portuguese). Division of Geol and Mineral, Department of National Mineral Production, Ministry of Agriculture, Monogr 13, Rio de Janeiro

Amundsen HEF (1987) Evidence for liquid immiscibility in the upper mantle. Nature 327: 692–695

Andersen T, Griffin WL, O'Reilly SY (1987) Primary sulfide melt inclusions in mantle-derived megacrysts and pyroxenites. Lithos 20: 279–294

Baker MB, Wyllie PJ (1990) Liquid immiscibility in a nepheline–carbonate system at 25 kbar and implication for carbonatite origin. Nature 346: 168–170

Brey GP, Koehler T (1990) Geothermobarometry in four-phase lherzolites. II New thermobarometers, and practical assessment of existing thermobarometers. J Petrol 31: 1353–1358

Dalton JA, Wood BJ (1993) The composition of primary carbonate melts and their evolution through wallrock reactions in the mantle. Earth Planet Sci Lett 119: 511–525

Dautria JM, Dupuy C, Takherist D, Dostal J (1992) Carbonate metasomatism in the lithospheric mantle: peridotitic xenoliths from a melilitic district of the Sahara basin. Contrib Mineral Petrol 111: 37–52

Dernov-Pegarev VF, Malinin SD (1976) Solubility of calcite in high temperature aqueous solutions of alkali carbonate and the problem of the formation of carbonatites (in Russian). Geokh 5: 643–657 (Translated in Geochem Int 13: 1–13)

Dickinson JE, Hess PC (1985) Rutil solubility and titanium coordination in silicate melts. Geochem Cosmochim Acta 49(11): 2289–2296

Edgar AD, Lloyd FE, Forsyth DM, Barnett RL (1989) Origin of glass in upper mantle xenoliths from the Quaternary volcanics

of Gees. West Eifel, Germany. Contrib Mineral Petrol 103: 277–286
Freestone IC, Hamilton DL (1980) The role of liquid immiscibility in the genesis of carbonatites. Contrib Mineral Petrol 73: 105–117
Hamilton DL, Kjarsgaard BA (1993) The immiscibility of silicate and carbonate liquids. S Afr J Geol 96: 139–142
Hamilton DL, Bedson P, Esson J (1989) The behaviour of trace elements in the evolution of carbonatites. In: Bell K (ed) Carbonatites: genesis and evolution. Unwin Hyman, London, pp 405–427
Hauri EN, Shimizu N, Dieu JJ, Hart SR (1993) Evidence for hot-spot-related carbonatite metasomatism in the oceanic upper mantle. Nature 365: 221–227
Hess HH (1960) Stillwater igneous complex Montana: a quantitative mineralogical study. Geol Soc Am Mem 80: 230
Ionov D (1998) Trace element composition of mantle-derived carbonates and coexisting phases in peridotite xenoliths from alkali basalts. J Petrol 39: 1931–1941
Ionov DA, Dupuy C, O'Reilly SY, Kopylova MG, Genshaft YS (1993) Carbonated peridotite xenoliths from Spitsbergen: implications for trace element signature of mantle carbonate metasomatism. Earth Planet Sci Lett 119: 283–297
Ionov DA, Hofmann AW, Shimizu NJ (1994) Metasomatism induced melting in mantle xenoliths from Mongolia. J Petrol 35: 753–785
Kjarsgaard BA, Hamilton DL (1989) The genesis of carbonatites by immiscibility. In: Bell K (ed) Carbonatites: genesis and evolution. Unwin Hyman, London, pp 388–404
Kjarsgaard BA, Peterson TD (1991) Nepheline–carbonatite liquid immiscibility at Shombole volcano, East Africa. Mineral Petrol 43: 293–314
Klemme S, Vanderlaan SR, Foley SF (1995) Experimentally determined trace and minor element partitioning between clinopyroxene and carbonatite melt under upper-mantle conditions. Earth Planet Sci Lett 133(3–4): 439–448
Kogarko LN (1993) Geochemical characteristics of oceanic carbonatites from Cape Verde Islands. S Afr J Geol 96(3): 119–125
Kogarko LN (1996) Geochemical models of supergiant apatite and rare-metal deposits related to alkaline magmatism. Geochem Intl 33: 129–149
Kogarko LN, Slutsky AB (2001) Carbonate–silicate–sulfide liquid immiscibility (in Russian). Dokl Acad Sci (in press)
Kogarko LN, Kramm U, Grauert B (1983) New data on age and genesis of Lovozero alkaline rocks (Rb–Sr signature) (in Russian). Dokl Acad Sci USSR 268(4): 970–972
Kogarko LN, Plant DA, Henderson CMB, Kjarsgaard BA (1991) Na-rich carbonate inclusion in perovskite and calzirtite from the Guli Intrusive Ca-carbonatite, Polar Siberia. Contrib Mineral Petrol 109: 124–129
Kogarko LN, Henderson CMB, Pacheco H (1995) Primary Ca-rich carbonatite magma and carbonate–silicate–sulfide liquid immiscibility mantle. Contrib Mineral Petrol 121: 267–274
Kogarko LN, Henderson M, Ntaflos T, Slutsky AB, Pacheco A (1998) Carbonate metasomatism of oceanic lithosphere and carbonate–silicate–sulfide liquid immiscibility. Mineral Mag 62A(2): 797–798
Kolesov GM (1994) Determination of trace elements: neutron-activation analysis in geochemistry and cosmochemistry. J Anal Chem 49(1): 50–58
Koster van Groos AF (1975) The effect of high CO_2 pressure on alkalic rocks and its bearing on the formation of alkalic ultrabasic rocks and the associated carbonatites. Am J Sci 275: 163–185
Kurat G, Palme H, Embey-Isztin A, Touret J, Ntaflos T, Spettel B, Brandstätter F, Palme C, Dreibus G, Prinz M (1993) Petrology and geochemistry of peridotites and associated vein rocks of Zabargad Island, Red Sea. Egypt Mineral Petrol 48: 309–341
Lee W-J, Wyllie PJ (1994) Experimental data bearing on liquid immiscibility, crystal fractionation and the origin of calciocarbonatites and natrocarbonatites. Int Geol Rev 36: 797–819
Lee W-J, Wyllie PJ (1996) Liquid immiscibility in the join $NaAlSi_3O_8$–$CaCO_3$ to 2.5 GPa and the origin of calciocarbonatite magmas. J Petrol 37: 1125–1152
Loomis TP, Gottschalk RR (1981) Hydrothermal origin of mafic layers in alpine-type peridotites: evidence from the Seiad Ultramafic Complex, California, USA. Contrib Mineral Petrol 76: 1–11
Menzies MA, Hawkesworth CJ (1987) Mantle metasomatism. Academic Press, London
Menzies MA, Murthy VR (1980) Nd and Sr isotope geochemistry of hydrous mantle nodules and their host alkali basalts: implications for local heterogeneities in metasomatically veined mantle. Earth Planet Sci Lett 46: 77–85
Menzies MA, Wass SY (1983) CO_2- and LREE-rich mantle below eastern Australia: a REE and isotopic study of alkaline magmas and apatite-rich mantle xenoliths from the Southern Highlands Province, Australia. Earth Planet Sci Lett 65: 287–302
Meyer HOA, Svisero DP (1987) Mantle xenoliths in South America. In: Nixon PH (ed) Mantle xenoliths. Wiley, Chichester, pp 85–93
Minarik WG (1998) Complications to carbonate melt mobility due to the presence of an immiscible silicate melt. J Petrol 39(11–12): 1965–1973
Mitchel-Thome RC (1970) Geology of the South Atlantic Islands. Gebrüder Borntraeger, Berlin
Pyle JM, Haggerty SE (1994) Silicate–carbonate liquid immiscibility in upper-mantle eclogites: implications for natrosilicic and carbonatitic conjugate melts. Geochim Cosmochim Acta 58: 2997–3011
Roedder E (1984) Fluid inclusions in minerals. Rev Mineral 12: 109–148
Rosenbaum JM, Zindler A, Rubenstone JL (1996) Mantle fluids: evidence from fluid inclusions. Geochim Cosmochim Acta 60: 3229–3252
Rudnick RL, McDonough WF, Chappell BW (1992) Carbonatite metasomatism in the northern Tanzanian mantle: petrographic and geochemical characteristics. Earth Planet Sci Lett 114: 463–475
Ryabchikov ID, Brey G, Kogarko LN, Bulatov VK (1989) Partial melting of carbonated peridotite at 50 kbar (in Russian). Geokh 1: 3–9
Schiano P, Clocchiatti R, Joron JL (1992) Melt and fluid inclusions in basalts and xenoliths from Tahaa Island. Society Archipelago: evidence for a metasomatised upper mantle. Earth Planet Sci Lett 111: 69–82
Schrauder M, Navon O (1994). Hydrous and carbonatitic mantle fluids in fibrous diamonds from Jwaneng, Botswana. Geochim Cosmochim Acta 58(2): 761–771
Seifert W, Thomas R (1995) Silicate–carbonate immiscibility: a melt inclusion study of olivine melilitite and wehrlite xenoliths in tephrite from the Elbe Zone, Germany. Chem Erde 55: 263–279
Shapkin AI, Garanin AV, Khodakovskii IL (1986) DIANIK GEOKHI. Russian Acad. Sci. Computer complex for chemical thermodynamics project. In: Direct and inverse thermodynamic tasks (in Russian). Nauka, Novosibirsk, pp 80–88
Silva LC, Le Bas MS, Robertson L (1981) An oceanic carbonatite volcano on Santiago, Cape Verde Islands. Nature 294: 644–645
Taylor SR, McLennan SM (1985) The continental crust: its composition and evolution. Blackwell, Oxford
Thibault Y, Edgar A, Lloyd FE (1992) Experimental investigation of melts from a carbonated phlogopite lherzolite: implications for metasomatism in the continental lithospheric mantle. Am Mineral 77: 784–794
Varella ME, Clocchiatti R, Kurat G, Schiano P (1999) Silicic glasses in hydrous and anhydrous mantle xenoliths from Western Victoria, Australia: at least two different sources. Chem Geol 153: 151–169
Veksler IV, Keppler H (2000) Partitioning of Mg, Ca, and Na between carbonatite melt and hydrous fluid at 0.1–0.2 GPa. Contrib Mineral Petrol 138(1): 27–34

Veksler IV, Nielsen TFD, Sokolov SV (1998) Mineralogy of crystallized melt inclusions from Gardiner and Kovdor ultramafic alkaline complexes: implications for carbonatite genesis. J. Petrol 39: 2015–2031

Wanke H, Baddenhausen H, Dreibus G, Jagoutz E, Kruse H, Palme H, Spettel B, Teschke F (1973) Multielement analyses of Apollo 15, 16 and 17 samples and the bulk composition of the moon. Geochem Cosmochim Acta (Suppl 4, vol 2): 1461–1481

Wallace ME, Green DH (1988) An experimental determination of primary carbonatite magma composition. Nature 335: 343–346

Wass SY, Rogers NW (1980) Mantle metasomatism – precursor to continental alkaline volcanism. Geochim Cosmochim Acta 44: 1199–1206

Wyllie PJ (1987) Discussion of recent papers on carbonated peridotite, bearing on mantle metasomatism and magmatism. Earth Planet Sci Lett 82: 391–397

Wyllie PJ (1989) Origin of carbonatites: evidence from phase equilibrium studies. In: Bell K (ed) Carbonatites: genesis and evolution. Unwin Hyman, London, pp 500–545

Wyllie PJ, Huang W-L (1976) Carbonation and melting reactions in the system $CaO–MgO–SiO_2–CO_2$ at mantle pressure with geophysical and petrological applications. Contrib Mineral Petrol 54: 79–107

Yaxley GM, Green DH (1998) Phase relations of carbonated eclogite under upper mantle PT conditions – implications for carbonatite petrogenesis. In: Extended abstracts of the 7th Kimberlite conference. Red Roof Design, Cape Town, pp 983–985

Yaxley GM, Green DH, Kamenetsky V (1998) Carbonatite metasomatism in the southeastern Australian lithosphere. J Petrol 39: 1917–1930

Yaxley GM, Crawford AJ, Green DH (1991) Evidence for carbonatite metasomatism in spinel peridotite xenoliths from western Victoria, Australia. Earth Planet Sci Lett 107: 305–317